

# The Significance of Interchannel Correlation, Phase and Amplitude Differences on Multichannel Microphone Techniques

Geoff Martin

Presented at the 113th International Convention of the Audio Engineering Society,  
Preprint no. 5671. Los Angeles, USA, 5 - 8 October, 2002.

## Abstract

There is a measurable interference between correlated signals produced by multiple loudspeakers in a standard five-channel loudspeaker configuration, resulting in an audible comb filter effect. This is due to small individual differences in distances between the ears of the listener and the various loudspeakers. Although this effect is caused by the dimensions and characteristics of the monitoring environment, it can be minimized in the recording process, particularly through the relative placement of microphones and choice of their directional characteristics. In order to analyse this effect, the correlation of microphone signals and their amplitude differences in a recording environment are evaluated using theoretical models. This procedure is applied to coincident and spaced pairs of transducers for direct and reverberant sounds.

## 1 Introduction

When a signal is combined with a delayed copy of itself, the result is called an *Finite Impulse Response (FIR) comb filter* [15]. Periodic modulation of the delay time produces a related effect commonly known in music production as *flanging* [25]. There are many situations where such a frequency response pattern is created, one of which is the interference between multiple coherent sound sources such as two loudspeakers situated at different distances from a listener. Although the ITU BS. 775-1 recommendation states that all five loudspeakers in a surround sound configuration should be equidistant from a listener, this is only possible when measuring from a single point – typically the centre of the listener’s head.

Unfortunately, since one’s ears are not located at this point, each loudspeaker actually has its own unique distance to the receiver. Consequently, when two or more loudspeakers are producing signals with a high degree of correlation at similar amplitudes, the result is a measurable comb filter with possible modulation caused by movement of the listener. This interference between multiple loudspeakers has been well documented for two-channel playback systems [9] [17] [26] [27] [2] [1] and a standard 5-channel configuration [12].

The audibility of this comb filtering effect can be reduced or eliminated either by increasing the interchannel amplitude difference or by decorrelating the signals produced by the two sources. When recording acoustic sources in real spaces, these can be controlled through careful attention to microphone choice and placement.

For the purposes of this investigation, we will use the ITU recommendation BS.775-1 for a five-channel reproduction system as shown in Figure 1. This consists of five full-range loudspeakers located at  $0^\circ$ ,  $\pm 30^\circ$  and  $\pm 110^\circ$  all equidistant to the listener [8]. (In fact, the specification allows for the surround loudspeakers to be symmetrically located within a range of  $\pm 100^\circ$  to  $\pm 120^\circ$ .)

Table 1 shows the calculated differences in the time of arrival of various loudspeaker pairs in a five-channel configuration with a loudspeaker distance of 140 cm from the listener with a head width of 14 cm. These calculations are based on straight paths from loudspeaker to ear position and do not include head diffraction effects. Included in this table are the corresponding frequencies of the lowest notch in the resulting comb filter effect.

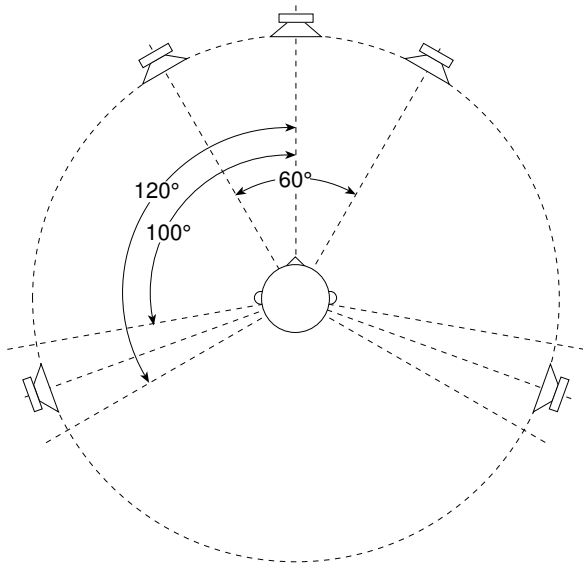


Figure 1: ITU BS. 775-1 Recommended loudspeaker configuration [8]

Loudspeaker Pair	Range of $\Delta t$ (Time of Arrival in $\mu\text{sec}$ )	Range of Lowest Notch Freq. (Hz)
L/R	172.4 - 203.5	2457 - 2901
C/L	77.1 - 105.3	4747 - 6488
C/R	72.0 - 105.3	4747 - 6946
C/LS	29.9 - 305.7	1636 - 16732
C/RS	28.2 - 298.4	1676 - 17714
L/LS	0.0 - 205.3	2435 - $\infty$
R/RS	0.0 - 195.5	2558 - $\infty$
LS/RS	328.3 - 382.4	1307 - 1523

Table 1: Calculated ranges of differences in times of arrival and frequencies of the lowest comb filter notch at the left ear from two loudspeakers with head rotation ranging from  $-30^\circ$  to  $30^\circ$  [12].

Table 2 lists the minimum interchannel amplitude differences required to ensure that this comb filter effect will be inaudible by a listener located in the “sweet spot” and rotating the head from  $-30^\circ$  to  $30^\circ$ , thus modulating the time of arrival difference between loudspeaker pairs. For example, in order to ensure that there is no perceivable comb filtering in a signal produced simultaneously by the Centre and Left loudspeakers, an attenuation of at least 20 dB must be applied to one of the two channels.

Loudspeaker Pair	$T$ (Minimum required amplitude difference)
C/L	20 dB
C/LS	25 dB
L/LS	23 dB
L/R	19 dB

Table 2: Minimum amplitude difference  $T$  between pairs of loudspeakers that are required to ensure that the comb filter effect caused by interference in the listening position is inaudible [12].

Alternatively, rather than ensuring adequate amplitude separation between the output channels, the correlation of the two sound sources could be reduced. The closer the interchannel correlation coefficient approaches 0, the smaller the perceived timbral distortion of the signals.

It is the goal of this investigation to evaluate the interchannel amplitude, phase and correlation characteristics for various microphone choices and configurations with particular attention paid to this issue of interference effects in the monitoring environment.

## 2 Microphone Polar Patterns

A microphone has an angle-dependent sensitivity pattern that is determined by the relative contributions of its pressure and pressure gradient components. This sensitivity is typically expressed using a two-dimensional model as is shown in Equation 1.

$$S_\alpha = P + G \cos \alpha \quad (1)$$

where  $S_\alpha$  is the sensitivity of the microphone at angle  $\alpha$ ,  $P$  is the pressure component contribution,  $G$  is the pressure gradient contribution and where  $P + G = 1$  [25].

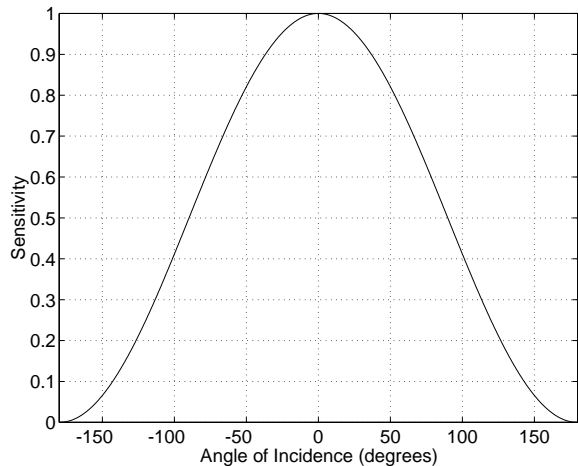


Figure 2: An example of the sensitivity pattern of a cardioid microphone using only the horizontal angle of incidence  $\sigma$ .  $P = 0.5$ ,  $G = 0.5$ .

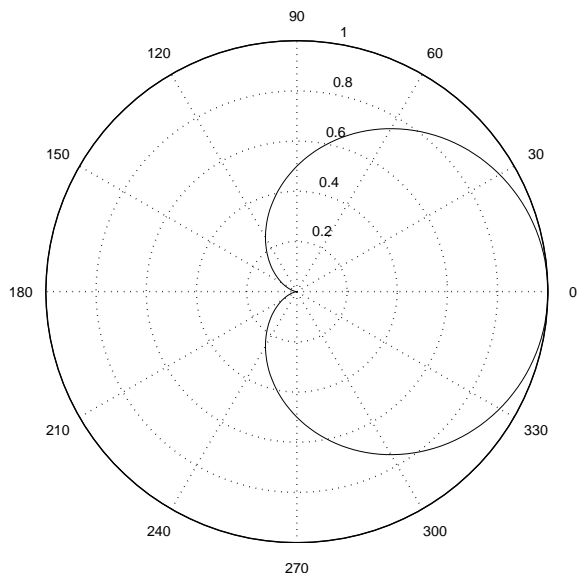


Figure 3: A polar representation of the same information presented in Figure 2.

In cases where  $P > 0.5$ , the polarity of the sensitivity at all angles of incidence is positive. Where  $P < 0.5$ , the polar pattern of the microphone will include an area commonly known as the “rear lobe” that produces a polarity inversion of the signal.

More often than not, microphones are used in a

three-dimensional space. Consequently, for the purposes of this investigation, it is necessary to consider this polar pattern using a horizontal angle of rotation  $\vartheta$  in addition to an angle of elevation  $\phi$  in a geographical coordinate system as is shown in Figure 4 and Equation 2.

$$S_{\{\vartheta, \phi\}} = P + G \cos \vartheta \cos \phi \quad (2)$$

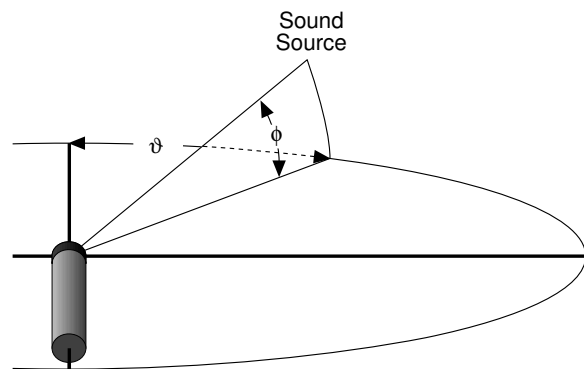


Figure 4: A three-dimensional view of a microphone showing the angle of rotation of the sound source to the pair  $\vartheta$ , and the elevation angle of the sound source  $\phi$ .

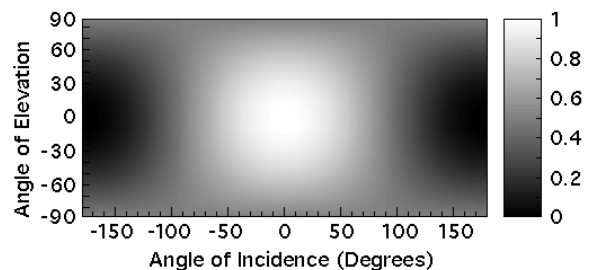


Figure 5: An example of the sensitivity pattern of a cardioid microphone using the horizontal angle of rotation  $\vartheta$  as well as the vertical angle  $\phi$ .

## 2.1 3-D Polar Coordinate Systems

Some discussion should be made here regarding the issue of different three-dimensional polar coordinate systems. Microphone polar patterns in three dimensions are typically described using the *spherical coordinate system* which uses two angles referenced to the origin on the surface of the sphere at the location  $(0, 0)$ . The first,  $\alpha$ , is an angle of rotation in the horizontal axis around the centre

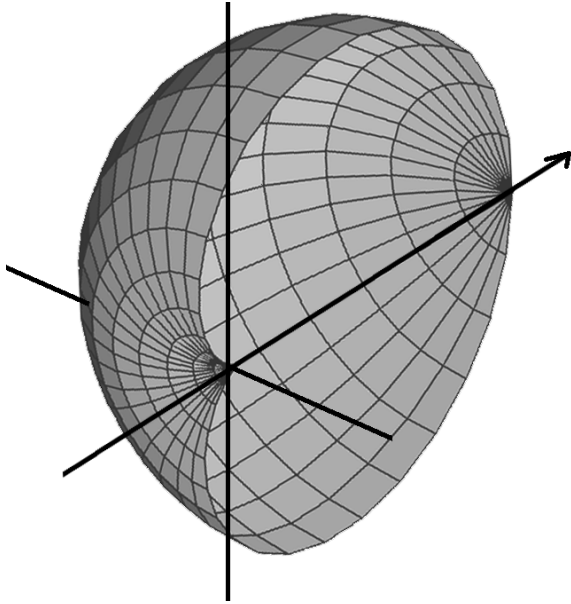


Figure 6: A three-dimensional polar plot of the sensitivity pattern of a cardioid microphone showing one half of the rotation.

of the sphere. The second,  $\delta$ , is an angle of rotation around the axis intersecting the centre of the sphere and the origin. This is shown on the right in Figure 7. In the case of microphones, the origin is thought of as being located at the centre of the diaphragm of the microphone and the axis for the rotation  $\delta$  is perpendicular to the diaphragm.

The *geographic coordinate system* also uses two angles of rotation. Similar to the spherical coordinate system, the first,  $\vartheta$ , is a rotation around the centre of a sphere in the horizontal plane from the origin at the location (0,0). In geographic terms, this would be the measurement of longitude around the equator. The second angle,  $\phi$ , is slightly different in that it is an orthogonal rotation off the equator, also rotating around the sphere's centre. The geographic equivalent of this vertical rotation is the latitude of a location as can be seen on the left in Figure 7.

This investigation uses the geographic coordinate system for its evaluation in order to make the explanations and figures more intuitive. For example, when a recording engineer places a microphone pair in front of an ensemble and raises the microphone stand, the resulting change in polar location of the instruments relative to the array is a change in elevation in the geographic coordinate

system. These changes in the angle of elevation of the microphone pair can correspond to changes in  $\phi$  up to  $\pm 90^\circ$ .

One issue to note in the use of the geographic coordinate system is the location of positions with values of  $\phi$  outside the  $\pm 90^\circ$  window. It must be kept in mind that these positions produce an alternation from left to right and vice versa. Therefore  $\vartheta = 45^\circ, \phi = 180^\circ$  is in the same location as  $\vartheta = -135^\circ, \phi = 0^\circ$

Although the use of the geographic coordinate system makes the figures and discussion of microphone pair characteristics more intuitive, this unfortunately comes at the expense of a somewhat increased level of complexity in the calculations.

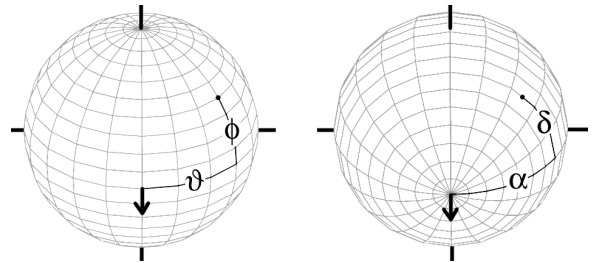


Figure 7: A comparison of the geographic and spherical coordinate systems. The point  $(\vartheta, \phi)$  in the geographic coordinate system shown on the left is identical to the point  $(\alpha, \delta)$  in the spherical coordinate system on the right.

### 3 Correlation Coefficient

The term “correlation” is one that is frequently misused and, as a result, misunderstood in the field of audio engineering. Consequently, some discussion is required to define the term. Generally speaking, the *correlation* of two audio signals is a measure of the relationship of these signals in the time domain [6]. Specifically, given two two-dimensional variables (in the case of audio, the two dimensions are amplitude and time), their *correlation coefficient*,  $r$  is calculated using their covariance  $\overline{s_{xy}}$  and their standard deviations  $\overline{s_x}$  and  $\overline{s_y}$  as is shown in Equation 3 [18]. The line over these three components indicates a time average, as is discussed below.

$$r = \frac{\overline{s_{xy}}}{\overline{s_x} * \overline{s_y}} \quad (3)$$

The *standard deviation* of a series of values is an indication of the average amount the individual values are different from the total average for all values. Specifically, it is the square root of the average of the squares of the differences between the average of all values and each individual value. For example, in order to find the standard deviation of a PCM digital audio signal, we begin by finding the average of all sample values. This will likely be 0 since audio signals typically do not contain a DC offset. Each sample is then individually subtracted from this average and each result is squared. The average of these squares is calculated and its square root is the standard deviation. When there is no DC component in an audio signal, its standard deviation is equal to its RMS value. In such a situation, it can be considered the square root of the average power of the signal.

The *covariance* of two series of values is an indication of whether they are interrelated. For example, if the average temperature for today's date is 19° C and the average humidity is 50%, yet today's actual temperature and humidity are 22° C and 65%, we can find whether there is an interdependent relationship between these two values, called the *covariation* [18]. This is accomplished by multiplying the differences of today's values from their respective averages, therefore  $(19 - 22) * (50 - 65) = 45$ . The result of this particular calculation, being a positive number, indicates that there is a positive relationship between the temperature and humidity today – in other words, if one goes up, the other does also. Had the covariation been negative, then the relationship would indicate that the two variables had behaved oppositely. If the result is 0, then at least one of the variables equalled the average value. The covariance is the average of the covariations of two variables measured over a period of time. The difficulty with this measurement is that its scale changes according to the scale of the two variables being measured. Consequently, covariance values for different statistical samples cannot be compared. For example, we cannot tell whether the covariance of air temperature and humidity is greater or less than the covariance of the left and right channels in a stereo audio recording if both have the same polarity.

Fortunately, if the standard deviations of the two signals are multiplied, the scale is identical to that of the covariance. Therefore, the *correlation coefficient* (the covariance divided by the product of the two standard deviations) can be considered to be a normalised covariance. The result is a value that can range from -1 to 1 where 1 indicates that the two signals have a positive linear relationship (in other words, their slopes always have the same polarity). A correlation coefficient of -1 indicates that the two signals are negatively linearly related (therefore, their slopes always have opposite polarities). In the case of wide-band signals, a correlation of 0 usually indicates that the two signals are either completely unrelated or separated in time by a delay greater than the averaging time.

In the particular case of two sinusoidal waveforms with identical frequency and a constant phase difference  $\omega\tau$ , Equation 3 can be simplified to Equation 4 [13].

$$r = \cos(\omega\tau) \quad (4)$$

where the *radian frequency*  $\omega$  is defined in Equation 5 [16] and where  $\tau$  is the time separation of the two sinusoids.

$$\omega \triangleq 2\pi f \quad (5)$$

where the symbol  $\triangle$  denotes “is defined as” and  $f$  is the frequency in Hz.

Further investigation of the topic of correlation highlights a number of interesting points. Firstly, two signals of identical frequency and phase have a correlation of 1. It is important to remember that this is true regardless of the amplitudes of the two signals [19]. Two signals of identical frequency and with a phase difference of 180° have a correlation of -1. Signals of identical frequency and with a phase difference of  $\pm 90^\circ$  have a correlation of 0. Finally, it is important to remember that the correlation between two signals is highly dependent on the amount of time used in the averaging process.

## 4 Free Field Analysis

A *free field* is a theoretical acoustic environment in which the wavefronts are free to expand outwards to infinity without encountering any scattering or reflecting surface or object [13]. In more typical situations, the direct sound and, in some cases, the earliest reflections in a large space as well as sources in acoustically absorptive environments can be individually simplified as sound sources in a free field. Using this model, sound sources can therefore be assumed to be in an anechoic environment. We are also assuming that the wavefront has travelled enough distance to be considered to be a plane wave – an assumption that may not necessarily hold true in real spaces.

### 4.1 Coincident directional microphones

Coincident microphone techniques provide differences in sensitivity of the microphones for a given angle of incidence resulting in level differences in the signals between the output channels [25]. These level differences produce different angular locations in the phantom image positions in the sound stage [14] [5]. The interchannel amplitude difference can be calculated using the sensitivity equations for the microphones, the so-called *included angle*  $\pm\Omega$  of the microphone pair, and the *angle of incidence* of the sound source to the pair, comprised of the angles of rotation  $\vartheta$  and elevation  $\phi$ . Figure 8 shows an example of the left microphone in a typical stereo pair.

Using a three-dimensional model where the included angle of the microphone pair is located on the horizontal plane, the sensitivity of the microphone can be calculated using Equation 6.

$$S_{n\{\vartheta,\phi,\Omega\}} = P_n + G_n \cos(\vartheta - \Omega_n) \cos \phi \quad (6)$$

The angle  $\Omega$  of a microphone can have a positive or negative value where a positive value indicates a clockwise rotation when the pair is viewed from above. Therefore, in the example of an XY pair of coincident cardioid microphones with an included angle of  $90^\circ$ , the right-facing microphone has a

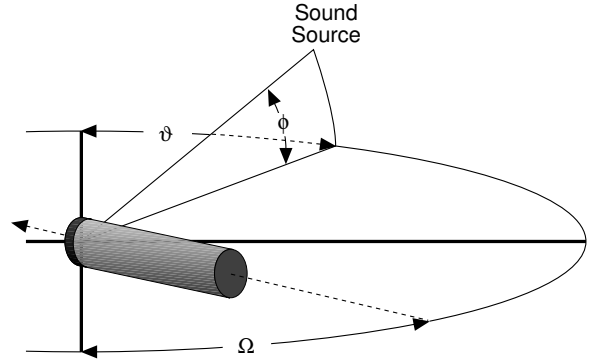


Figure 8: A three-dimensional view of a microphone showing the microphone angle of rotation,  $\Omega$ , the angle of rotation of the sound source to the pair  $\vartheta$ , and the elevation angle of the sound source  $\phi$ .

value of  $\Omega = 45^\circ$ , the left-facing microphone has a value of  $\Omega = -45^\circ$ .

The difference in sensitivity between two coincident microphones can be calculated on a decibel scale using Equation 7. The absolute value is used in this calculation to circumvent the issue of negative values of  $\frac{S_1}{S_2}$  for specific angles of incidence and some polar patterns. As a result, this equation does not indicate areas where opposite polarities are produced by the two microphones.

$$\Delta S = 20 \log_{10} |R| \quad (7)$$

where the ratio of the sensitivities of the microphones,  $R$  is calculated using Equation 8

$$R = \frac{S_1}{S_2} \quad (8)$$

The evaluation of the influence of coincident directional microphones on the amplitude difference and correlation of their output signals is most easily carried out by subdividing their directional characteristics into two categories. The first is the case of microphones with a value of  $P \geq 0.5$ . The second is the case of transducers with a value of  $P < 0.5$ .

#### 4.1.1 $P \geq 0.5$

This category includes omnidirectional microphones ( $P = 1$ ), subcardioids ( $P = 0.75$ ) and cardioids ( $P = 0.5$ ). As was previously stated, microphones with a pressure component of 0.5 or greater exhibit the characteristic that the polarity of the sensitivity at all angles of incidence is either 0 (in the case of a single angle of incidence where  $P = 0.5$ ) or positive (for all other polar patterns where  $P > 0.5$ ).

#### Amplitude differences

Figure 9 shows the theoretical sensitivity differences of a pair of cardioid microphones with an included angle of  $90^\circ$  and angles of rotation around the pair for the full  $360^\circ$  and an angle of elevation of  $0^\circ$ . This graph can be used in conjunction with the threshold of audibility of a comb filter for a given pair of loudspeakers to determine the angles of incidence of sound sources to the microphone pair which will result in timbral artifacts in the monitoring room. This is the set of all angles of incidence where  $-T < \Delta S < T$ . For example, if we use the 20 dB minimum amplitude difference for the Centre/Left loudspeaker pair from Table 2, the angles of incidence where a  $90^\circ$  pair of coincident cardioids will produce audible artifacts are those that result in sensitivity differences between -20 dB and 20 dB. In this particular case, this area is comprised of all angles of rotation where  $-103^\circ < \theta < 103^\circ$  and  $155^\circ < \theta < 205^\circ$ . Also note that generally, the closer  $\Delta S$  is to 0 dB, the more audible the comb filter.

Changing the configuration of the microphone pair will alter the size of these angular regions. For cardioids, the more the included angle approaches  $180^\circ$  the narrower the problem area. This can be seen in Figure 10 which shows a contour plot of a pair of cardioid microphones with  $-180^\circ \leq \vartheta \leq 180^\circ$ ,  $\phi = 0^\circ$  and  $0^\circ \leq \pm\Omega \leq 180^\circ$ . A number of sensitivity differences are plotted ranging from 0 dB to  $\pm 24$  dB in 6 dB increments. This range includes values close to the suggested values of  $T$  in Table 2. However, since these values were found using single channel diotic stimuli presented over headphones and since it has been estimated that binaurally presented stimuli would result in a loss of sensitivity to the comb filter on the order of 10 dB [26], the contours for smaller differences are also plotted. Finally, the 0 dB contour is shown as

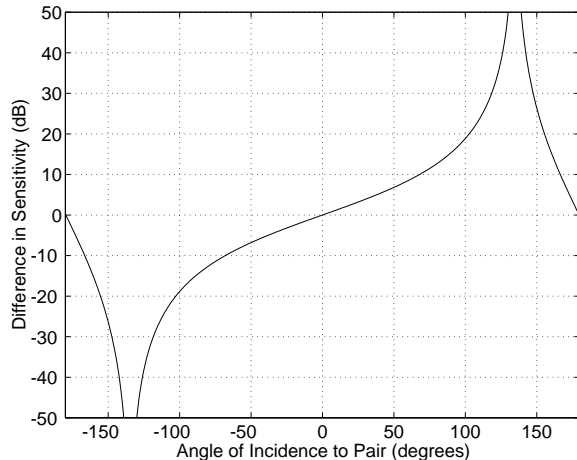


Figure 9: An example of the difference in sensitivity  $\Delta S$  between two coincident cardioid microphones with an included angle of  $90^\circ$  and a sound source elevation of  $0^\circ$

a “worst-case” location. Figure 9 can be thought of as a vertical “slice” of Figure 10 for an included angle of  $90^\circ$ .

In the case of coincident microphones with pressure components of 0.5 or less, changes in elevation will also have an effect on the relative amplitudes of the signals. As can be seen in Figures 11 and 12, as the value of  $\phi$  goes from  $0^\circ$  to either  $-90^\circ$  or  $90^\circ$ , the interchannel amplitude difference goes to 0 dB. This is true for all included angles with the exception of  $\pm\Omega = 0^\circ$ , where all angles of rotation and elevation result in  $\Delta S = 0$  dB.

This issue is important not only in this investigation but in the question of phantom image location between the loudspeakers. For example, in cases where a coincident pair of cardioids is placed in front of an ensemble and the microphone stand is subsequently raised, the amplitude difference between the channels will be lowered with two effects: the audibility of the interchannel interference will increase, and the the width of the ensemble in the playback soundfield will collapse.

Similar plots have not been shown for coincident omnidirectional and subcardioid microphones. This is due to the fact that the theoretical sensitivity difference for omnidirectionals at all angles of incidence is 0 dB regardless of the included angle. Similarly, the highest possible sensitivity difference for subcardioid microphones (which occurs at

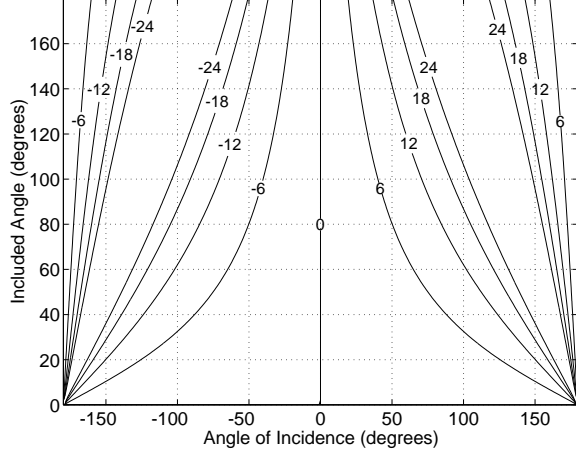


Figure 10: Contour plot showing the difference in sensitivity in dB between two coincident cardioid microphones with included angles of  $0^\circ$  to  $180^\circ$ , angles of rotation from  $-180^\circ$  to  $180^\circ$  and a  $0^\circ$  angle of elevation. Note that Figure 9 is a horizontal “slice” of this contour plot where the included angle is  $90^\circ$ .

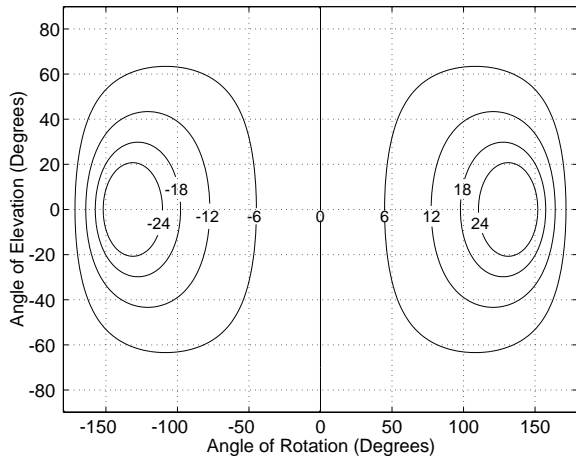


Figure 11: Difference in sensitivity between two coincident cardioid microphones with an included angle of  $90^\circ$ , angles of rotation from  $-180^\circ$  to  $180^\circ$  and angles of elevation from  $-180^\circ$  to  $180^\circ$ .

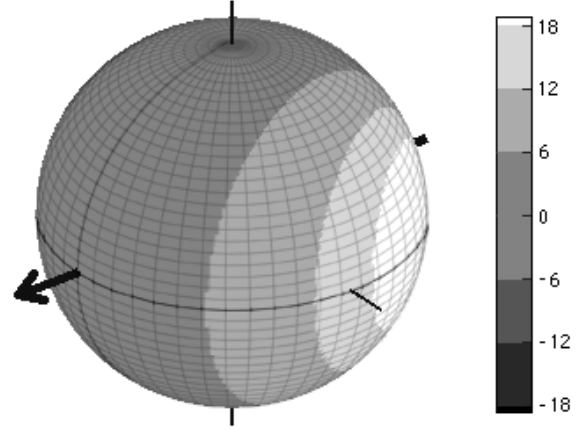


Figure 12: The contour plot shown in Figure 11 mapped onto a spherical representation. The boundaries between filled shades are at  $\pm 6$  dB,  $\pm 12$  dB and  $\pm 18$  dB. The scale on the right is in decibels.

an included angle of  $180^\circ$ ) is 6 dB. Consequently, all included angles result in audible comb filtering at all angles of rotation and elevation.

### Correlation

A wavefront arriving at a coincident pair of microphones will reach both transducers simultaneously, therefore there are no phase differences between the two outputs regardless of the angle of incidence of the sound source. Consequently, the covariance of the outputs of the two microphones for a sound source at a given angle of incidence is directly proportional to the product of their two sensitivities for that angle. Similarly, the effect of each individual sensitivity on the standard deviation of the microphone’s output can be found using the square root of the square of the sensitivity – in effect, its absolute value. The result is the correlation coefficient shown in Equation 9.

$$r_{\{\vartheta, \phi\}} = \frac{S_1 S_2}{\sqrt{S_1^2} \sqrt{S_2^2}} \quad (9)$$

where  $r_{\{\vartheta, \phi\}}$  is the correlation coefficient of the outputs of a pair of coincident microphones 1 and 2 at a single angle of rotation and elevation. Microphone 1 has an angle-dependent sensitivity of  $S_1$  and microphone 2 has an angle-dependent sensitivity of  $S_2$ .

Since, in the particular case of a pair of microphones where  $P > 0.5$ , the two signals are identical in every respect with the exception of level, Equation 9 can be simplified to Equation 10.

$$r_{\{\vartheta, \phi\}} = 1 \quad (10)$$

In the particular case where at least one of the microphones has a cardioid polar pattern (when  $P = 0.5$ ), then there is at least one angle of incidence where the correlation of the two signals is 0. This is caused by the absence of signal at the null of the transducer.

Since the correlation coefficient for the signals from two coincident microphones in this category is always 1, we must rely on the amplitude difference in order to reduce the audibility of the interchannel interference in the monitoring environment.

#### 4.1.2 $P < 0.5$

This category includes supercardioid microphones, ( $P = 0.336$ ) hypercardioids ( $P = 0.75$ ) and bidirectionals ( $P = 0$ ) [25], however, only the latter two will be evaluated.

#### Amplitude differences

The sensitivity difference of two coincident directional microphones with negative rear lobes is evaluated in exactly the same manner as the procedure described above, using Equation 7. As can be seen in Figures 13 and 16, the primary difference in the response of these microphone pairs in the horizontal plane when compared to cardioids is that there are more subdivisions of the  $360^\circ$ . For example, in the case of cardioid microphones with any included angle, there are only two angles of incidence in the horizontal plane where  $\Delta S = 0$  dB,  $0^\circ$  and  $180^\circ$ . For bidirectional microphone pairs, there are four locations where the amplitude difference of the two output channels is 0 dB,  $0^\circ$ ,  $\pm 90^\circ$  and  $180^\circ$ . Note, however, that this particular analysis ignores the polarity difference of the signals at the sides of the pair. While this issue is of paramount importance in the issue of imaging of signals in the playback soundfield, it can be virtually ignored in this investigation [12].

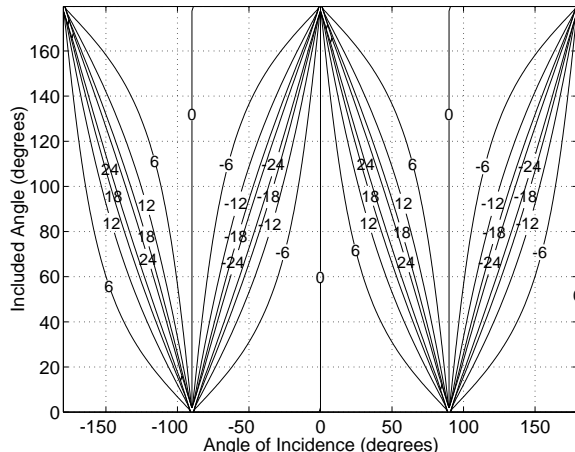


Figure 13: Contour plot showing the difference in absolute values of the sensitivities, expressed in dB between two coincident bidirectional microphones with included angles of  $0^\circ$  to  $180^\circ$ , angles of rotation from  $-180^\circ$  to  $180^\circ$  and a  $0^\circ$  angle of elevation.

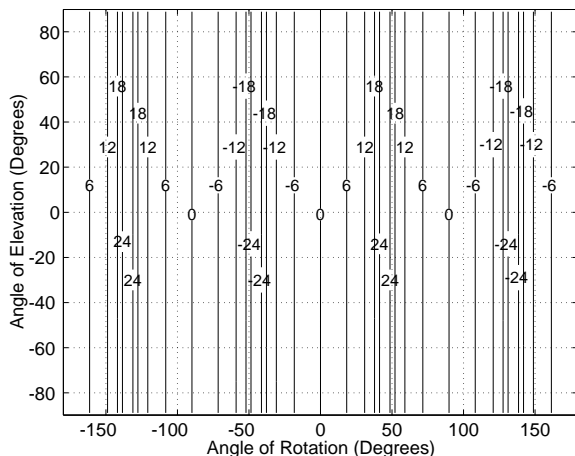


Figure 14: Difference in the absolute values of the sensitivities between two coincident bidirectional microphones, expressed in dB, with included angles of  $90^\circ$ , angles of rotation from  $-180^\circ$  to  $180^\circ$  and angles of elevation from  $-180^\circ$  to  $180^\circ$ .

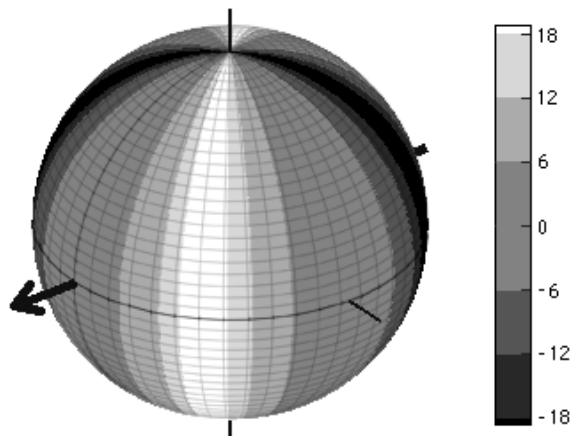


Figure 15: The contour plot shown in Figure 14 mapped onto a spherical representation. The boundaries shown between filled shades are at  $\pm 6$  dB,  $\pm 12$  dB and  $\pm 18$  dB. The scale on the right is in decibels.

Figures 14 and 15 show examples of a coincident pair of bidirectional microphones with an included angle of  $90^\circ$ . Similar to Figure 11, these are contour plots showing the sensitivity difference of the microphones for all angles of rotation and elevation. Note that changes in the angle of elevation of the sound source relative to the microphones pair do not change the interchannel sensitivity difference in this particular case. This characteristic is true for all coincident pairs of bidirectional microphones, regardless of the included angle. Consequently, changes in the height of the microphone stand will change neither the audibility of the comb filter effect, nor the image location of the direct sound from the instruments in the ensemble.

Figures 17 and 18 show examples of a coincident pair of hypercardioid microphones with an included angle of  $90^\circ$ . In the case of changes of elevation for pairs of hypercardioids, the behaviour is similar to that of cardioid pairs. As can be seen in Figure 17, as the angle of elevation moves away from  $0^\circ$ , the interchannel sensitivity difference is reduced for approximately the front  $140^\circ$  of the microphone pair, albeit not as significantly as is the case with cardioids with small changes in elevation. There are other areas around the microphone pair which behave differently, however. For example, sound sources within the area of approximately  $70^\circ < \vartheta < 120^\circ$  (and its symmetrical counterpart), result in *increases* in the interchan-

nel amplitude difference for small changes in elevation away from  $0^\circ$ .

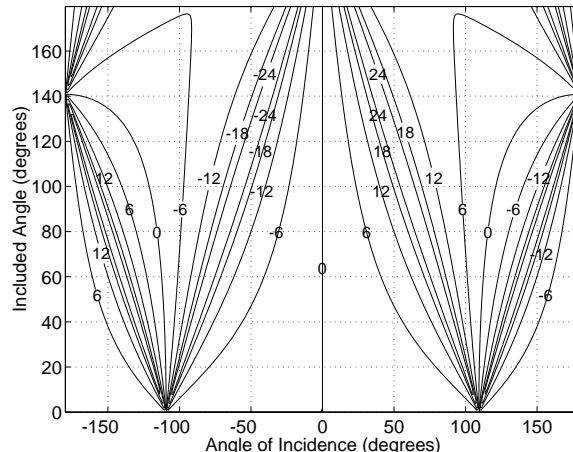


Figure 16: Contour plot showing the difference in absolute values of the sensitivities, expressed in dB between two coincident hypercardioid microphones with included angles of  $0^\circ$  to  $180^\circ$ , angles of rotation from  $-180^\circ$  to  $180^\circ$  and a  $0^\circ$  angle of elevation.

### Correlation

The use of at least one microphone with a pressure component of less than 0.5 produces a similar case to that discussed above for microphones where  $P \geq 0.5$ . The only difference lies in the polarity of the correlation coefficient caused by the polarity relationship between the two microphones at a given angle of incidence. For angles where the two polarities are alike, the correlation coefficient remains at 1. In the case of angles where the two polarities are opposite, the correlation coefficient is -1. Again, at angles of incidence where at least one of the sensitivities is 0, the correlation coefficient is 0. Equation 11 illustrates this property and, in fact, can be used as a general equation for all coincident microphone pairs, regardless of the value of  $P$ .

$$r_{\{\vartheta, \phi\}} = \text{sign}(S_1 S_2) \quad (11)$$

where  $\text{sign}(x)$  is a function indicating the polarity of the variable  $x$ .  $\text{sign}(x) = 1$  for all  $x > 0$ ,  $\text{sign}(x) = -1$  for all  $x < 0$ ,  $\text{sign}(x) = 0$  for all  $x = 0$ ,

Since the correlation of all coincident microphone

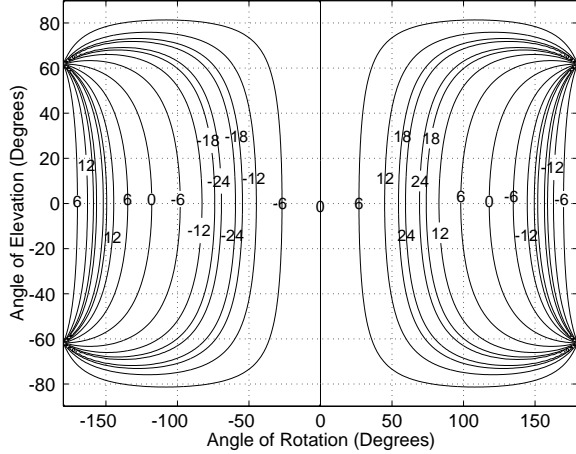


Figure 17: Difference in the absolute values of the sensitivities between two coincident hypercardioid microphones, expressed in dB, with included angles of  $90^\circ$ , angles of rotation from  $-180^\circ$  to  $180^\circ$  and angles of elevation from  $-180^\circ$  to  $180^\circ$ .

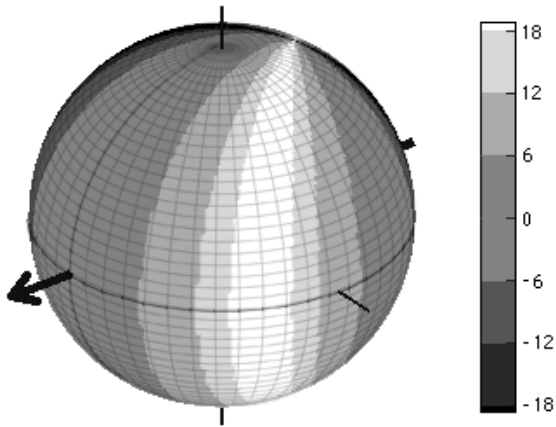


Figure 18: The contour plot shown in Figure 17 mapped onto a spherical representation. The boundaries shown between filled shades are at  $\pm 6$  dB,  $\pm 12$  dB and  $\pm 18$  dB. The scale on the right is in decibels.

pairs is either 1 or -1 in almost every situation, we must rely exclusively on interchannel sensitivity differences to reduce the audibility of comb filtering in the monitor location.

## 4.2 Spaced omnidirectional microphones

In the case of spaced omnidirectional microphones, it is commonly assumed that the distance to the sound source is adequate to ensure that the impinging sound can be considered to be a plane wave. In addition, it is also assumed that there is no difference in signal levels due to differences in propagation distance to the transducers. In reality, for widely spaced microphones and/or for sound sources closely located to any microphone, neither of these assumptions is correct, however they will be used for this investigation.

The difference in time of arrival of a sound at two spaced microphones is dependent both on the separation of the transducers  $d$ , the angle of rotation around the pair  $\vartheta$  and the angle of elevation to the pair  $\phi$ .

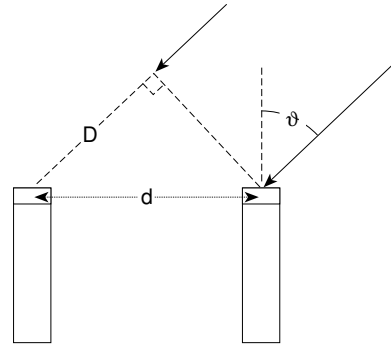


Figure 19: Spaced omnidirectional microphones showing the microphone separation  $d$ , the angle of rotation  $\vartheta$  and the resulting extra distance  $D$  to the further microphone. Note that the the angle of elevation  $\phi$  is not shown.

The additional distance travelled by the sound wave to the further of the two microphones, shown in Figure 19, can be calculated using Equation 12.

$$D = d \sin \vartheta \cos \phi \quad (12)$$

The result of this time of arrival difference caused

by the extra propagation distance is a frequency-dependent phase difference between the two channels. This interchannel phase difference  $\omega\tau$  can be calculated for a given additional propagation distance using Equation 13.

$$\omega\tau = \frac{2\pi D}{\lambda} \quad (13)$$

where  $\lambda$  is the acoustic wavelength in air.

This can be further adapted to the issue of microphone separation and angle of incidence by combining Equations 12 and 13, resulting in Equation 14.

$$\omega\tau_{\{\vartheta,\phi\}} = kd \sin \vartheta \cos \phi \quad (14)$$

where  $\omega\tau_{\{\vartheta,\phi\}}$  is the frequency-dependent phase difference between the channels for a sound source at angle of rotation  $\vartheta$ , angle of elevation  $\phi$ , and  $k$  is the acoustic wavenumber, defined in Equation 15 [13].

$$k \triangleq \frac{\omega}{c} \quad (15)$$

where  $c$  is the speed of sound in air.

The comb filtering effects experienced at the listening position are the result of frequency-dependent phase differences between the signals from two loudspeakers at the ears of the listener. If we assume that the two channels are identical and we simplify the listener's ear to an omnidirectional microphone, ignoring the effects of head shadowing and diffraction, the resulting frequency-dependent gain  $G_\tau$  of the direct sound caused by interference at the receiver can be calculated in decibels using Equation 16.

$$G_\tau = 20 \log_{10} [1 + \cos(\omega\Delta\tau)] \quad (16)$$

where  $\Delta\tau$  is the difference in the time of arrival of the signals from the two loudspeakers.

The phase difference  $\omega\tau_{\{\vartheta,\phi\}}$  caused by the difference in the time of arrival of a sound wave at

two spaced omnidirectional microphones will alter the frequency response characteristics of this interference at the listening position. Combining Equations 14 and 16 we obtain Equation 17.

$$G_{\{\tau,\vartheta,\phi\}} = 20 \log_{10} [1 + \cos(\omega\Delta\tau + kd \sin \theta \cos \phi)] \quad (17)$$

As can be seen in Figure 20, the result at the listening position when using spaced omnidirectional microphones is a simple modulation in the fundamental frequency of the comb filtering effect. The wider the microphone separation, and/or the closer the angle of rotation is to  $\pm 90^\circ$ , the lower the fundamental frequency of the filter.

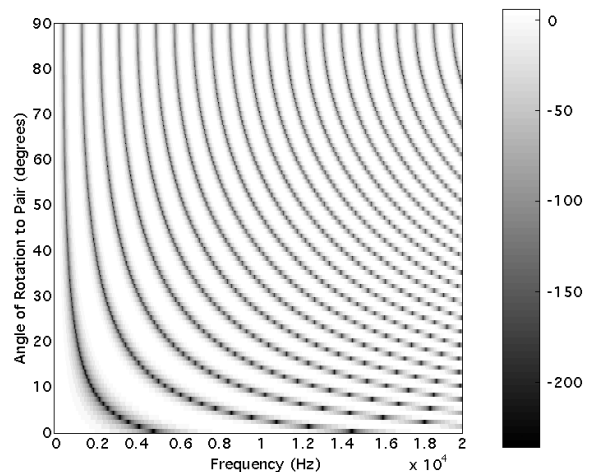


Figure 20: Theoretical total gain in dB resulting from the interference of two loudspeakers at the listening position, including phase differences caused by spaced omnidirectional microphones.  $\Delta\tau = 102.9\mu\text{sec}$ , equivalent to the delay difference between the Centre and Left loudspeakers at the left ear with a head rotation of  $0^\circ$  [12],  $d = 34.4\text{cm}$ ,  $\phi = 0^\circ$ .

It should be noted that this analysis does not consider one important issue related to the phase relationship of spaced microphones in real spaces: the effect of room modes on the phases of the two transducers. Resonant frequencies and standing waves in a real room, particularly in smaller enclosures, will have a dramatic effect on this behaviour.

## 5 Diffuse Field Analysis

Unlike a free field in which the wavefront arrives at the receiver from a single predictable direction, a perfect *diffuse field* is one where the wavefront has an equal probability of arriving from every direction. In practice, this does not mean that sound arrives from all directions simultaneously. It does, however, mean that sound will arrive from every direction within a given time window. If we consider a typical situation, a reverberant space will continuously approach a diffuse field state throughout its impulse response. Consequently, the reverberant tail is usually considered and modeled as a diffuse field. Although this assumption is an oversimplification, it will be used for the purposes of this investigation.

### 5.1 Coincident Directional Microphones

A pair of coincident directional microphones in a diffuse field can be considered on an intuitive level as an extension of the corresponding configuration in a free field. Again, we shall subdivide this transducer arrangement into two subsections.

#### 5.1.1 $P \geq 0.5$

If we consider that a diffuse field is comprised of an infinite number of sound waves arriving from all directions at the microphone pair, but that each of these will have a correlation coefficient of 1 in a pair of coincident microphones with pressure components of greater than 0.5, then the average correlation of all sound waves is 1. Consequently, any coincident pair of omnidirectionals, subcardioids or cardioids will have a correlation coefficient of 1 at all times in a reverberant space.

In the case of a diffuse field, the outputs of the microphones can be subdivided into two categories using the threshold of audibility of the comb filter as the dividing line. Angles of rotation and elevation that result in interchannel sensitivity differences within the threshold are problematic – those that produce differences outside the threshold are not. The angle of elevation  $\phi_R$  of this border where the threshold  $T$  (in dB) is equal to  $\Delta S$

at a given angle of rotation can be calculated using Equations 18 and 19. These assume that the microphones have matched polar patterns and an included angle  $\pm\Omega$ . The result of this equation is the contour plotted in the first quadrant in Figure 11 for a given value of  $T$  where  $0 \leq \vartheta \leq 180^\circ$ .

$$R = 10^{\frac{|T|}{20}} \quad (18)$$

The theoretical total output power of a microphone in a diffuse field based only on its polar pattern, commonly called the *Random-Energy Response* or *RER*, is calculated by finding the square of the surface area of its three-dimensional polar pattern. This is commonly calculated using the spherical coordinate system as is shown in Equation 20 [25].

$$RER = \int_0^\pi \int_0^{2\pi} S^2 \sin \alpha \, d\delta \, d\alpha \quad (20)$$

where  $S$  is the sensitivity of the microphone at angle of incidence  $\alpha$  and  $\delta$  is the angle of rotation around the microphone's axis.

Instead of using Equation 20, the RER of a microphone can be calculated in the geographic coordinate system as is shown in Equation 21.

$$RER = 2 \int_0^{2\pi} \int_0^{\frac{\pi}{2}} S^2 \cos \phi \, d\phi \, d\vartheta \quad (21)$$

In order to determine the total power output of each microphone in the coincident pair for angles of rotation and elevation where  $\Delta S$  is outside the threshold  $\pm T$ , Equation 21 is modified to obtain Equation 22.

The total power output of each microphone in the coincident pair for angles of rotation and elevation where  $\Delta S$  is within the threshold  $\pm T$ , can be calculated using Equation 23.

$$B_n = RER_n - A_n \quad (23)$$

The ratio of  $A_{tot}$  to  $B_{tot}$ , expressed in decibels, is calculated using Equation 24.

$$\phi_R = \Re \arccos \left| \frac{-P(1-R)}{\cos(\Omega - \vartheta) - P \cos(\Omega - \vartheta) - R \cos(\Omega + \vartheta) + PR \cos(\Omega + \vartheta)} \right| \quad (19)$$

$$A_n = 2 \left[ \int_0^\pi \int_0^{\phi_R} (S_{n\{\vartheta, \phi, \Omega\}})^2 \cos \phi d\phi d\vartheta + \int_0^\pi \int_0^{\phi_R} (S_{n\{\vartheta, \phi, -\Omega\}})^2 \cos \phi d\phi d\vartheta \right] \quad (22)$$

$$C = 10 \log_{10} \left[ \frac{A_{tot}}{B_{tot}} \right] \quad (24)$$

where  $A_{tot} = A_1 + A_2$  and  $B_{tot} = B_1 + B_2$ .

When  $C = 0$  dB, the summed power output of the two microphones comprising signals outside the threshold  $\pm T$  is equal to that of signals within the threshold. The lower the value of  $C$ , the higher the likelihood that the comb filtering effect at the monitoring position will be audible. When  $C = -\infty$  dB, there are no signals outside the threshold of audibility.

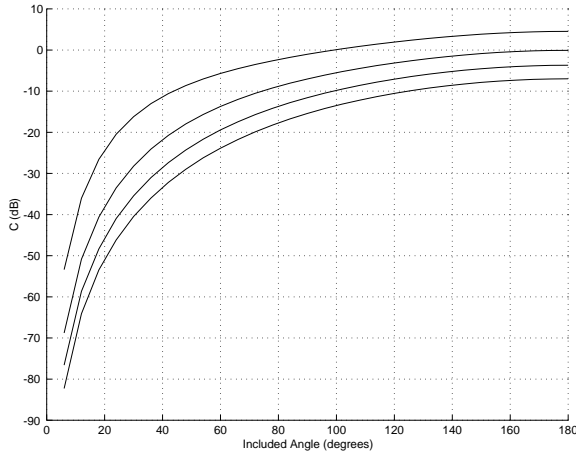


Figure 21: Value of  $C$  for included angles from  $0^\circ$  to  $180^\circ$  for a pair of cardioid microphones for various threshold levels. From top to bottom,  $T = 6$  dB, 12 dB, 18 dB and 24 dB.

Figure 21 shows values of  $C$  for various included angles and four different thresholds. These plots were created using matrices of discrete values calculated in MATLAB rather than using the continuous functions described above. As can be seen, the ratio of summed powers outside  $\pm T$  to those within  $\pm T$  increases as the included angle approaches

$180^\circ$ . Consequently, the comb filter at the monitoring position becomes less audible. Also note that values of  $T$  greater than approximately 12 dB cannot result in values of  $C$  as high as 0 dB.

### 5.1.2 $P < 0.5$

The behaviour of a pair of coincident microphones where at least one of the microphones has a negative polarity rear lobe can be intuitively considered in the same manner as in the previous section. In this case, however, the sound waves arriving at the microphone pair will have a correlation of -1, 0, or 1, depending on the angles of incidence of the sound source and the included angle of the microphones.

Unfortunately, it is slightly more difficult to calculate the value of  $C$  in this configuration. This is due to the fact that Equation 22 assumes that the boundary line created by  $\phi_R$  forms an angle no greater than  $90^\circ$  with the equatorial plane. As can be seen in Figure 17, this is not the case for pairs of hypercardioid microphones.

As in the case of Figure 21, the value of  $C$  for supercardioid and hypercardioid microphones was calculated numerically using MATLAB. These values are plotted in Figures 22 and 23.

Figure 22 shows the value of  $C$  for various included angles and threshold levels for a pair of supercardioid microphones. Note that it is possible to obtain higher values of  $C$  for lower values of  $T$  at included angles approaching  $180^\circ$  than it is with cardioid microphones. However, higher values of  $T$  do not exhibit this characteristic. This is likely due to the presence of the relatively insensitive rear lobe of the microphone whose effective contribution increases as  $T$  approaches 0 dB.

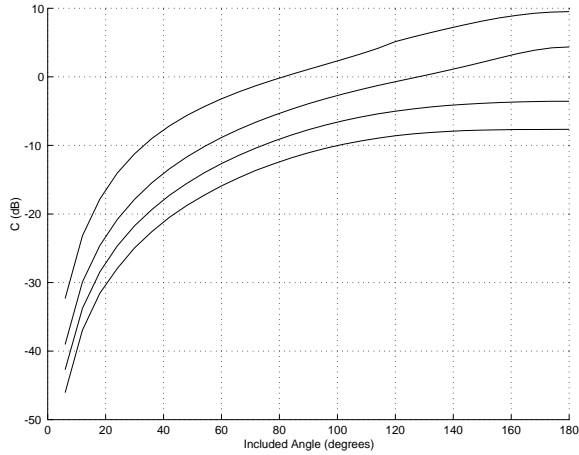


Figure 22: Value of  $C$  for included angles from  $0^\circ$  to  $180^\circ$  for a pair of supercardioid microphones for various threshold levels. From top to bottom,  $T = 6$  dB, 12 dB, 18 dB and 24 dB.

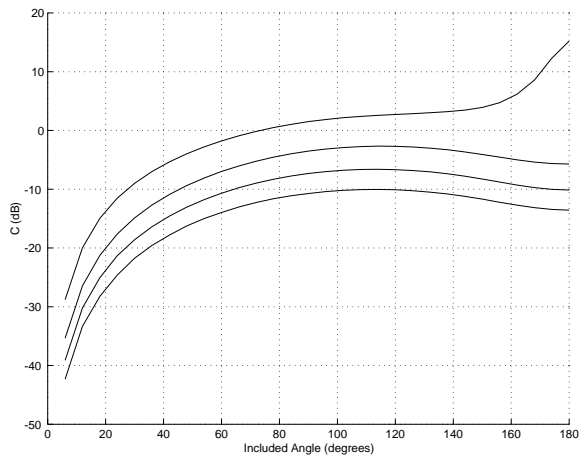


Figure 23: Value of  $C$  for included angles from  $0^\circ$  to  $180^\circ$  for a pair of hypercardioid microphones for various threshold levels. From top to bottom,  $T = 6$  dB, 12 dB, 18 dB and 24 dB.

Figure 23 shows the values of  $C$  for various included angles and threshold levels for a pair of hypercardioid microphones. Two interesting characteristics are seen here. Firstly, as in the case of the supercardioids, there is a large increase in the value of  $C$  for the 6 dB threshold level when the included angle nears  $180^\circ$ . This is again due to the contributions of the rear lobe. Secondly, the higher threshold levels begin to exhibit a characteristic of falling off for larger included angles. This is similar to the extreme case that will be seen in the evaluation of bidirectional microphones. The practical result of this characteristic is that, unlike all other polar patterns, the included angle which produces the maximum value of  $C$  is different for different threshold levels.

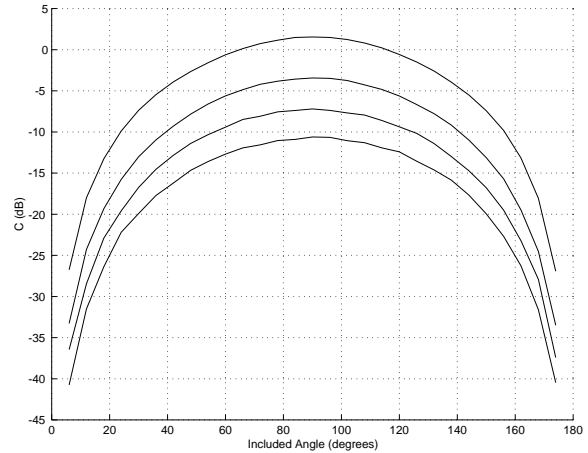


Figure 24: Value of  $C$  for included angles from  $0^\circ$  to  $180^\circ$  for a pair of bidirectional microphones for various threshold levels. Top to bottom,  $T = 6$  dB, 12 dB, 18 dB and 24 dB.

Pairs of pure bidirectional microphones can be considered a subset within this category due to their specific characteristic that any change in  $\phi$  have no effect on differences in sensitivity between the microphones. This can be seen in Figures 14 and 15. Bidirectional microphones show a symmetrical characteristic for the value of  $C$ , mirrored at an included angle of  $90^\circ$  – a textbook “Blumlein” configuration, shown in Figure 24. This is due to the fact that the front and rear lobes of the bidirectional microphones have equal sensitivities.

## 5.2 Spaced Omnidirectional Microphones

Two omnidirectional microphones placed in a perfect diffuse field will produce similar output levels and a frequency-dependent correlation coefficient that is determined solely by their separation,  $d$ . This correlation can be calculated using Equation 25.

$$r_d = \frac{\sin(kd)}{kd} \quad (25)$$

where  $r_d$  is the frequency-dependent correlation coefficient of two sound pressures  $p_1$  and  $p_2$  at two different points separated by distance  $d$  in a three-dimensional perfect diffuse field [10] [13].

This equation assumes that the space is diffuse in all three dimensions. In cases where both microphones are located in the plane of a two-dimensional diffuse field, the correlation coefficient is calculated using a 0<sup>th</sup>-order Bessel function and is dependent upon the frequency and microphone separation [10]. In situations where the microphones are perpendicular to the two-dimensional plane of diffusion, the correlation coefficient is 1 for all frequencies [10]. These two-dimensional situations are not evaluated in this investigation due to the relative lack of similar real-world situations. Note, however, that these characteristics would indicate a change in the correlation of spaced microphones in a diffuse field with changes in the directional characteristics of the transducers.

Figure 25 shows the correlation coefficient vs. frequency for a pair of omnidirectional microphones with an arbitrary separation of 34.4 cm in a diffuse field. This can be used to make general comments regarding the relationship of the outputs of the microphones. As can be seen, the correlation approaches 1 at low frequencies and approaches 0 at high frequencies. A more general model, shown in Figure 26 may be more useful.

Figure 26 shows the relationship between the correlation coefficient of spaced omnidirectional microphones and the ratio of the acoustic wavelength to the transducer separation. Not surprisingly, as can be seen from Equation 25 and Figure 26, the longest wavelength where  $r_d = 0$  is where the mi-

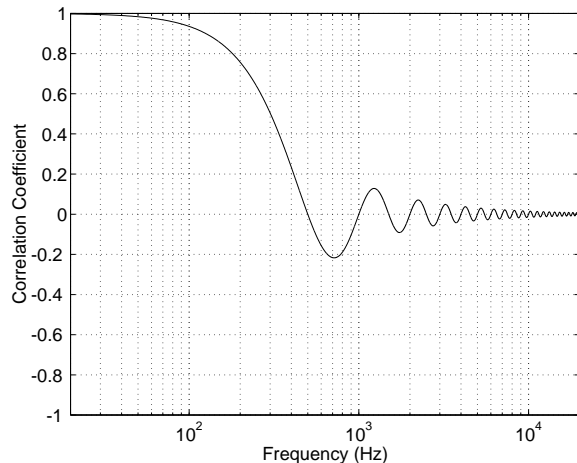


Figure 25: Theoretical correlation coefficient vs. frequency for a pair of perfectly omnidirectional microphones with a separation of 34.4 cm in a perfect diffuse field.

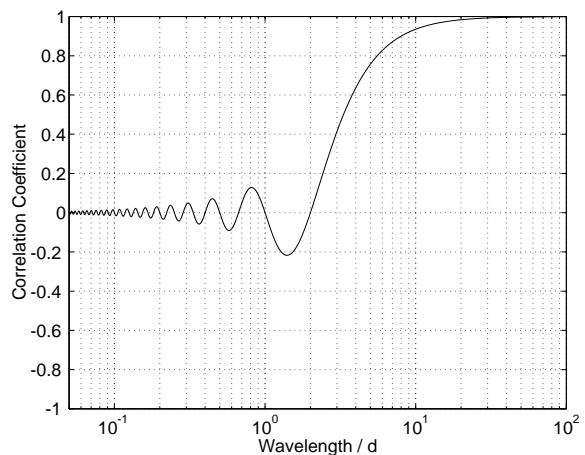


Figure 26: Theoretical correlation coefficient vs. ratio of wavelength to microphone separation for a pair of perfectly omnidirectional microphones in a perfect diffuse field.

crophones are separated by  $\frac{\lambda}{2}$ .

Unfortunately, it is impossible to combine the frequency-dependent correlation coefficient in this model with the known FIR comb filter at the listening position in order to determine the resulting effect on the interference pattern. We can, however, make a number of general statements regarding this relationship. Firstly, at low frequencies, particularly where  $d$  is approximately less than  $\frac{\lambda}{2}$ , any audible comb filter effects caused by the monitoring environment will not be reduced. Using the lowest calculated notch frequency listed in Table 1, approximately 1.3 kHz, we can conclude that the minimum permissible microphone separation should be at least 13.2 cm. Although this separation is smaller than that typically recommended for spaced microphone techniques, it should be noted that listeners located away from the sweet spot will require decorrelation at lower frequencies and therefore larger microphone separations.

Secondly, the sum of two noise sources with a correlation coefficient of 0 produces a simple power sum resulting in a gain of 3 dB (assuming that both signals have the same power level) with no periodic frequency-dependent interference. As a result, frequency components in the diffuse field above approximately  $d = \lambda$  cannot produce audible comb filtering effects in the monitoring environment.

As in the case of the free field analysis of omnidirectional microphones, there are a number of real-world acoustical issues which have been omitted from this analysis. The issue of room modes has a larger effect on the low-frequency diffuse field response of the microphone pair than in a free field situation. This is because we are equating the reverberant tail with the diffuse field, thus concentrating on a later component in the impulse response, allowing more time for the resonant frequencies to develop. In larger rooms where the Schroeder Frequency [13] is likely quite low, and the microphone separation is small in relation, it is unlikely that there will be a large effect on the correlation coefficient. In smaller rooms, the effect will be much more noticeable. For example, it is possible to have a spaced pair of pressure microphones with a correlation coefficient approaching -1 at specific modal frequency centres if they are located in pressure antinodes of opposite polarity.

Secondly, it is assumed that the microphones are not located near any reflecting surfaces. Proximity to a wall in a reverberant space will change the correlation coefficient characteristics of the two signals by reducing the level of diffusion at frequencies dependent on the distance to the reflecting or absorbing surface [4].

## 6 Future Work

This investigation constitutes only the beginning of what is potentially a long chain of research on the issue of management of interchannel interference at the listening position in a multichannel playback environment. Much work remains to be accomplished in order to obtain a more complete understanding of some of the effects described herein.

Firstly, the issue of oversimplification of the direct and reverberant portions of the impulse response at the microphones to perfect free field and diffuse field situations must be addressed. It may be possible to apply weighting coefficients to the direct sound and reverberation based on the distance to the sound source from the microphones and the reverberation radius for the recording space in order to predict the relative contributions to interference artifacts at the listening position.

Secondly, although the value of  $C$  (described in Section 5) can be calculated, it is unknown what value is required for what threshold for various microphone choices and environments. It is likely that the temporal density of reflections in the reverberant tail will have an effect on the desired value for this variable. This avenue of research will require further listening tests to determine preferences for this balance of signals within and without the threshold of audibility of the comb filtering effect.

Thirdly, as was discussed above, the issues of room modes and proximity of the microphones to reflecting surfaces needs to be evaluated on a case-by-case basis.

Fourthly, this research is based on the assumption that every microphone has a perfect, frequency-independent polar pattern. Obviously, this is not the case in the real world. Although some inves-

tigations have shown the accuracy of theoretical predictions of characteristics such as the phase response of spaced omnidirectional microphones [3], there are far more cases where the real world departs radically from simple mathematics. Consequently, it will be necessary to undertake a series of measurements of real transducers in real spaces in order to determine a level of reliability of the theoretical models presented here.

## 7 Conclusions and Comments

As was stated in the introduction, the general concentration of this investigation is only on the timbral effects caused by interference between multiple channels in the monitoring environment. The imaging characteristics of sources in the reproduced sound stage have not been considered. Unfortunately, there will be many occasions where these two issues are in conflict. Consequently, the recording engineer must weigh the importance of each according to the situation and musical genre, either favouring one or the other, or compromising both. It is important to remember, however, that although there have been many studies which propose a “system” for mathematically determining microphone configurations [7] [20] [21] [11] [23] [24] [22], these typically exclusively examine the imaging characteristics of sources using a free field model. While such systems contribute greatly to the understanding of the response of microphone arrays, there are many issues other than image location which must be considered during the recording session. Ultimately, these can only be evaluated and balanced through careful listening.

## 8 Thanks

Special thanks to Philippe Depalle in the Music Technology Area, Jason Corey in the Sound Recording Area and Nilima Nigam in the Department of Mathematics and Statistics at McGill University, Bruce Bartlett of Crown International, Kypros Christodoulides at the Banff Centre, Søren Bech and Jan Abildgaard Pedersen at Bang & Olufsen a/s, Cassia Pole and Jennifer Stephenson for their assistance in the research and writing of this paper.

## References

- [1] J. C. Bennett; K. Barker and F. O. Edeko. A new approach to the assessment of stereophonic sound system performance. *Journal of the Audio Engineering Society*, 33(5):314–321, May 1985.
- [2] Jens Blauert. *Spatial hearing: the psychophysics of human sound localization*. MIT Press, Cambridge, 1983. Translated by John S. Allen.
- [3] Eddy Bøgh Brixen. Phase relation in stereo signals from dual microphone set-ups. In *96th Convention of the Audio Engineering Society, Preprint no. 3825*, Amsterdam, Netherlands, 26 February - 1 March 1994. Audio Engineering Society.
- [4] Lawrence E. Kinsler; A. R. Frey; A. B. Coppen and J. V. Sanders. *Fundamentals of acoustics*. Wiley, New York, 4th edition, 1999.
- [5] Geoff Martin; Wieslaw Woszczyk; Jason Corey and René Quesnel. Sound source localization in a five-channel surround sound reproduction system. In *107th Convention of the Audio Engineering Society, Preprint no. 4994*, volume 4994, New York, 24-27 September 1999. Audio Engineering Society.
- [6] Frank J. Fahy. *Sound intensity*. Elsevier Applied Science, London; New York, 1989.
- [7] David Griesinger. Griesinger’s coincident microphone primer. Cambridge, USA, 7 October 1985.
- [8] ITU. Multichannel stereophonic sound system with and without accompanying picture. Standard BS.775-1, International Telecommunication Union, 1992–1994 1994.
- [9] W. Koenig. Subjective effects in binaural hearing. *Journal of the Acoustical Society of America*, 22(1):61–62, January 1950.
- [10] Heinrich Kuttruff. *Room Acoustics*. Elsevier Applied Science. Elsevier Science Publishers, Essex, 3rd edition, 1991.
- [11] Geoff Martin. Towards a better understanding of stereo microphone technique. [www.tonmeister.ca/research](http://www.tonmeister.ca/research), 1996.

- [12] Geoff Martin. Interchannel interference at the listening position in a five-channel loud-speaker configuration. In *113th Convention of the Audio Engineering Society*, Los Angeles, 5 - 8 October 2002. Audio Engineering Society.
- [13] Christopher L. Morfey. *Dictionary of Acoustics*. Academic Press, San Diego, 2001.
- [14] Gert Simonsen. Master's thesis, Technical University of Denmark, Lyngby, 1984.
- [15] Kenneth Steiglitz. *A DSP primer: with applications to digital audio and computer music*. Addison-Wesley Pub., Menlo Park, 1996.
- [16] John Strawn, editor. *Digital Audio Signal Processing: An Anthology*. William Kaufmann, Inc., Los Altos, 1985.
- [17] Günther Theile. Weshalb ist der kammfiltereffekt bei summenlokalisation nicht hörbar? In *11. Tonmeister-Tagung*, pages 200–214, Berlin, 1978.
- [18] John Neter; William Wasserman and G.A. Whitmore. *Applied Statistics*. Allyn and Bacon, Boston, USA, 4th edition, 1992.
- [19] Deutsche Welle. Stereo recording techniques. [www.dwelle.de/rtc/infotheque](http://www.dwelle.de/rtc/infotheque).
- [20] Michael Williams. The stereophonic zoom - a variable dual microphone system for stereophonic sound recording. Bru sur Marne, France, 1990.
- [21] Michael Williams. Microphone arrays for natural multiphony. In *91st Convention of the Audio Engineering Society, Preprint no. 3157*, New York, USA, 4 - 8 October 1991. Audio Engineering Society.
- [22] Michael Williams. Multichannel microphone array design: Segment coverage analysis above and below the horizontal reference plane. In *112th Convention of the Audio Engineering Society, Preprint no. 5567*, Munich, Germany, 10 - 13 May 2002. Audio Engineering Society.
- [23] Helmut Wittek. Directional imaging using L-C-R microphones - theoretical and practical investigations. In *Proceedings of the 19th International Conference of the Audio Engineering Society*, pages 448–455, Schloss Elmau, Germany, 21 - 24 June 2001. Audio Engineering Society.
- [24] Helmut Wittek and Günther Theile. The recording angle based on localisation curves. In *112th Convention of the Audio Engineering Society, Preprint no. 5568*, Munich, Germany, 10 - 13 May 2002. Audio Engineering Society.
- [25] John M. Woram. *Sound Recording Handbook*. Howard W. Sams and Co., Indianapolis, 1st edition, 1989.
- [26] Patrick M. Zurek. Measurements of binaural echo suppression. *Journal of the Acoustical Society of America*, 66(6):1750–1757, December 1979.
- [27] Patrick M. Zurek. The precedence effect and its possible role in the avoidance of interaural ambiguities. *Journal of the Acoustical Society of America*, 67(3):952–964, March 1980.